

Flux trapping in hafnium-doped Y-Ba-Cu-O ceramics: The microwave-loss-signal analysis

A. G. Vedeshwar and H. D. Bist

Department of Physics, Indian Institute of Technology, Kanpur 208 016, India

S. K. Agarwal and A. V. Narlikar

National Physical Laboratory, New Delhi, India

(Received 8 June 1989; revised manuscript received 28 November 1989)

Studies of microwave absorption at low fields in zero-field-cooled (ZFC) and field-cooled (FC) samples of Hf-doped Y-Ba-Cu-O are presented. Flux trapping during the FC process is clearly demonstrated. Results show that the superconducting glass phase appears in ceramics for fields greater than or equal to H_m (where H_m is the field at which the signal is maximum), where the difference between ZFC and FC signals starts. The results can be explained quite satisfactorily in terms of a percolation description and the superconducting cluster model.

The microwave loss (or absorption) signal observed in new superconducting ceramics with¹⁻⁴ and without^{5,6} field modulation has been a sensitive probe to detect the superconducting transition,¹ grain size,^{6,7} aging effect,⁷ and impurity phases⁷ in the samples. Its origin is attributed to fluxon pinning and depinning in the critical state.^{8,9} However, microwave studies in FC samples are very scarce in the literature. A large difference in ZFC and FC studies has been observed by other measurements¹⁰⁻¹² and is interpreted in terms of a glass model¹⁰ or a flux-creep model.¹² ZFC and FC measurements are referred to as diamagnetic shielding and the Meissner effect, respectively. However, Giovannella *et al.*¹³ have shown that the FC procedure need not necessarily give a measure of the Meissner effect. Also it is reported¹⁴ that glassy effects are predicted for temperature between 70% and 95% of T_c and magnetic fields in the range of 0.03–0.2 T. Therefore, we have studied ZFC and FC Hf-doped 1:2:3 samples using a microwave loss signal with field modulation, to have a better understanding of the magnetic properties of these ceramics at very low fields.

Samples were prepared by a standard solid-state reaction method by firing and sintering the stoichiometric mixture of the oxides of Y, Ba, and Cu. Hafnium doping was effected by mixing an appropriate amount of hafnium oxide in the mixture. The detailed analysis of these samples is given elsewhere.⁷ Samples were well characterized by x-ray diffraction, scanning electron microscopy (SEM), density measurements, and resistivity measurements. T_c decreased by 2 K from 90 K as Hf doping was increased from 0.5% to 2%, but its density and mechanical strength increased and its aging effect and porosity were reduced.

Microwave loss signals were recorded using an EPR spectrometer (Varian E-109) in a standard conventional TE₁₀₂ configuration at a microwave frequency of 9.4 GHz. All the spectra shown here were recorded at 77 K using a homemade quartz Dewar. A pair of Helmholtz coils was used to nullify the remnant field of the EPR magnets and for negative direction of the field. The mag-

netic field was calibrated with an accuracy of ~ 0.05 mT using a highly sensitive digital Gaussmeter. Samples were ceramic and spherical in shape which were well polished and sealed in 3-mm-diameter quartz tubes. The recording conditions are specified for each figure. The same conditions were maintained for all spectra and an equal amount of samples were taken for the purpose of comparison.

Samples were cooled in an almost zero field (less than 0.01 mT) and then the ZFC spectrum was recorded. Since this is a differential signal ($d\chi''/dH$), the signal height (h_p) and peak position (H_m) are characteristics of the sample. The height determines the amount of change of the slope of the absorption versus the field curve at a certain characteristic field H_m . This is the advantage of the field modulation. In direct microwave absorption measurements such a change is difficult to notice. H_m is an important parameter and is identified as the lower intergranular critical field H_{c1J} in the Josephson-junction model⁸ which can be used to estimate Josephson penetration depth along the junction. H_m is also identified as H_{c1}^* in the superconducting cluster model² which can be used to calculate the superconducting cluster size. This signal depends upon the amplitude of the modulating field analogous to the amplitude of the ac field in ac susceptibility measurements. H_m can be used to estimate the grain size in the sample.⁷ As grain size decreases, H_m increases. The signal is reversible in both forward and reverse directions of the field if the field is scanned up to H_m which shows that this field can be identified as H_{c1J} . For $H > H_{c1J}$, Josephson vortices begin to appear and are trapped¹⁴ which is evident by the area swept by the loop when the field is scanned to $H > H_m$. The amount of trapped flux depends on the scanning field, impurities in the sample, and defects (etc.). The vortex self energy or energy per vortex line can also be calculated by H_m ($\epsilon \simeq \phi_0 H_m a / 4\pi \simeq E_J$ where a is grain size¹⁵). All the three quantities, namely, signal height, peak position, and the amount of trapped flux decrease with increasing temperature and vanish around T_c .¹⁶

More interesting results are obtained in the case of FC samples cooled at different fields. Samples were cooled from the normal state to 77 K in the desired field and then the spectra were recorded. To compare the results, the field was scanned to the same value and all recording conditions were kept identical. Figure 1 shows the actual recorded signals in ZFC (topmost curve) and FC samples. The field at which the sample was cooled is indicated at each signal. It can be noted that the signal does not change appreciably up to the cooling field less than or equal to H_m . For higher cooling fields the height and area under the loop (ΔA) decreases while the peak position (H_m) shifts to higher fields. All three of these parameters are shown as a function of cooling field (H_{FC}) in Figs. 2 and 3. Signal height increases up to the cooling field equal to H_m and then decreases. For fields more than 5 mT it becomes saturated. Similar behavior is observed in the variation of H_m with H_{FC} , but the peak position remains almost constant up to the cooling field equal to H_m . The variation of the amount of trapped flux (the area under the signal loop) with the cooling field is shown in Fig. 3. This behavior is similar to that of h_p and H_m in all three samples. All three parameters are proportionate to the percentage of doping. The ac losses can be reduced by pinning the fluxes. Therefore, reduction in the signal height must be proportional to the trapped flux as observed here. The decrease in h_p for the 2 at. % Hf-doped sample, which should have been greater than the 1 at. % Hf-doped sample, is somewhat puzzling. However, at present we can not comment on this. Fur-

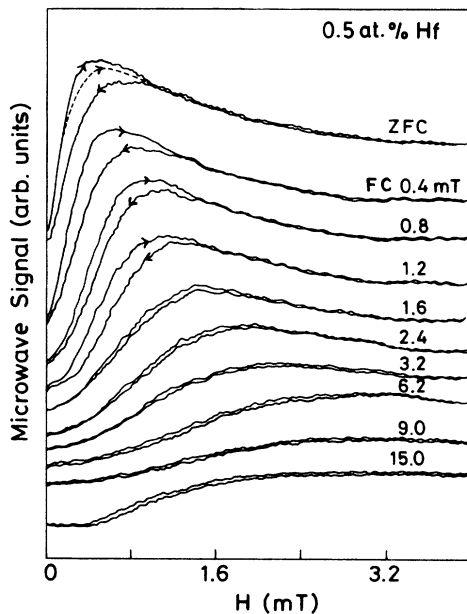


FIG. 1. Actual recorded microwave loss signals of ZFC and FC samples at 77 K. Recording conditions were modulation amplitude—0.1 mT at 100 kHz, microwave power — 0.2 mW, and gain—1000. The field at which the sample was cooled is specified at each FC curve. The broken curve in ZFC represents the second scan after exposing it to 4 mT.

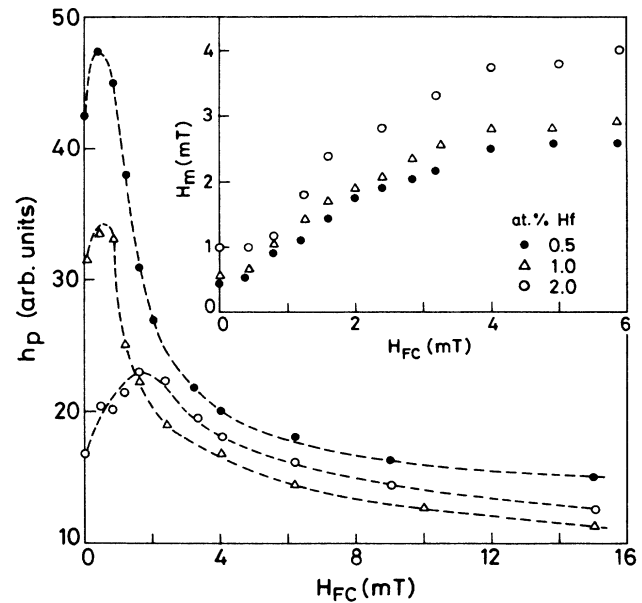


FIG. 2. Signal height (h_p) as a function of the cooling field (H_{FC}) for the three samples with different Hf doping. Inset shows the variation of the peak position (H_m or H_{c1j}) with the cooling field.

ther, by trapping the flux between the grains, some of the very weakly coupled grains are decoupled, and the net area of the superconducting loop projected normal to the applied field is reduced, and the area is inversely proportional to H_m ($S = \phi_0/2H_m$, where S is the superconducting loop area²). Therefore, a shift in H_m towards the higher field, as observed, is expected. ΔA decreases as the cooling field is increased because there is already trapped flux during FC as evident by the reduction in height and signal retraces for repeated scans. The height of the signal also decreases in the second scan after ex-

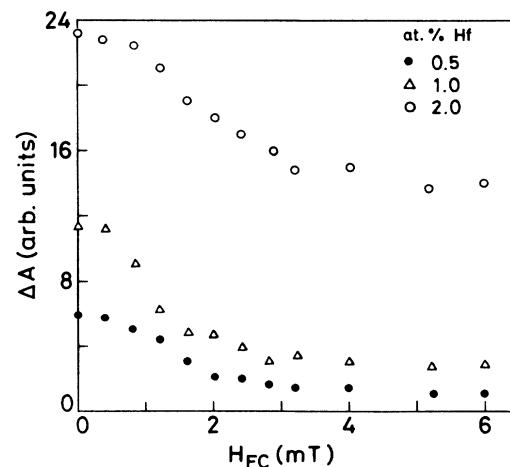


FIG. 3. Variation of the amount of trapped flux (area under the signal loop, ΔA) with the cooling field for the three samples.

posing the ZFC sample to the field greater than H_m (shown by a broken curve in Fig. 1). The results, however, are not identical in ZFC and FC cases.

If we expose the FC sample to the negative field some of the trapped fluxes are depinned. We have illustrated this fact in Fig. 4. After cooling the sample in a field of 4 mT, the signal was recorded. The subsequent spectra shown in the figure were recorded after exposing the sample to different negative fields (specified at each spectrum). It can be seen that the signal recovers towards the ZFC signal. By exposure to negative fields, some of the trapped fluxes are released so that the height of the signal increases, the peak position shifts towards lower fields, and ΔA increases. These parameters are shown in Fig. 5 as a function of the exposed negative field. If we expose the FC sample to the negative field equal to the cooling field, all the trapped fluxes are not depinned. There is a remnant trapped flux in the sample which accounts for the difference between the ZFC and FC processes. This may be due to the inhomogeneous coupling strengths between different grains in the sample arising from the inhomogeneous sizes of the grains.

The superconducting properties of granular systems are well explained in terms of the percolation model^{17,18} or superconducting cluster model.¹⁹ According to these models the coupling between superconducting grains is established through the Josephson interaction when coupling energy E_j exceeds the thermal energy; that is, E_j decreases with increasing temperature. When the cou-

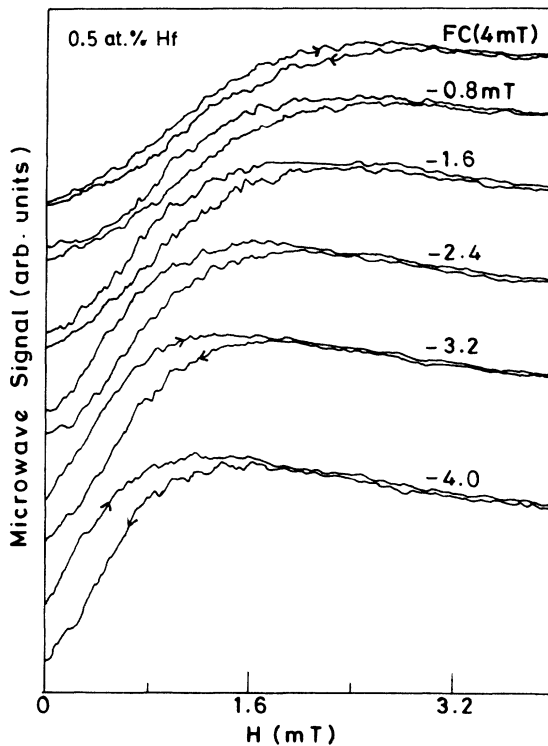


FIG. 4. Effect of negative field exposure on the FC sample which demonstrates the depinning of the fluxes. Recording conditions were the same as specified in Fig. 1, but the gain, however, was 2000.

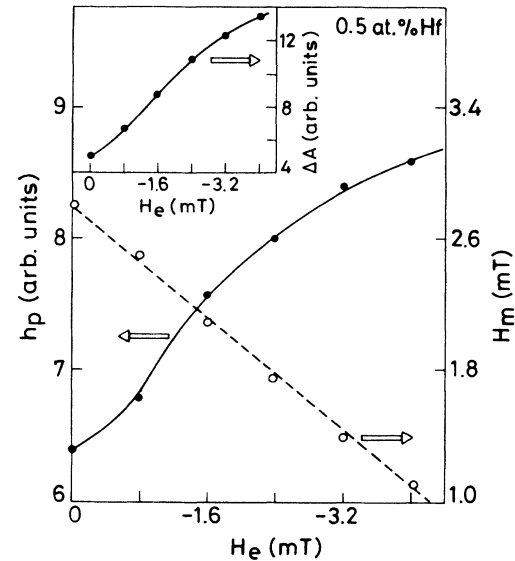


FIG. 5. The measured parameters (defined in Figs. 2 and 3) of the signals of Fig. 4 as a function of the negative field (H_e) exposure.

pling probability equals the percolation threshold at a particular temperature an infinite cluster of superconducting grains is formed. However, if normal state resistance of the sample is high, the charging energy must be considered where E_j has to exceed the thermal plus charging energy to form the clusters. In our samples normal state resistance varies from $1.8 \text{ m}\Omega$ (at 0.5 at. % Hf) to $2.3 \text{ m}\Omega$ (at 2 at. % Hf) and electrostatic effects (charging energy) can be neglected. Also, our resistivity measurements⁷ show the monotonic resistivity decreasing with temperature (metallic) suggesting the weak links between the grains. For weak links, charging energy is negligible.¹⁷ By analyzing the normal-state resistivity of our samples using percolation description¹⁷ we see that T_c which is observed experimentally, is hardly affected—that is, T_c is decreased nominally by one or two degrees at 2 at. % Hf doping. Our results are very consistent with the model which predicts the increase in the width of the electrical transition as normal state resistivity becomes larger—an effect which has been observed in our resistivity measurements. Recently, it was shown²⁰ that percolation probability is directly proportional to the temperature by comparing temperature dependent resistivity and susceptibility with those of simulations using a bond percolation model. Moreover, it has been shown that susceptibility transition starts only after resistivity goes to zero, i.e., for $p \geq p_c$.

Our results can be understood better using the theory of Ebner and Stroud for diamagnetic response of weakly linked superconducting clusters. This theory also explains the glassy behavior observed at low fields. The key to this model is frustration which means that at finite fields, any cluster with closed loops can not find a state that simultaneously minimizes all the bond energies. A largely frustrated cluster with many closed loops can choose between numerous competing ground states with

nearly equal energy. In a finite cluster, only one of these is the true ground state and others will lie only a small energy above it. The various levels will cross one another as the field is varied and the cluster must hop from one configuration to another in order to stay in the ground state. The projected area of cluster can be calculated by the relation,¹⁹ $S = \phi_0 / 2H_{c1}^*$ where H_{c1}^* is the field at which the first flux slippage occurs or clusters become weakly random. The peak position H_m of the low-field signal can be identified² as H_{c1}^* . Using this relation the variation of cluster diameters as a function of the cooling field is obtained from the inset of Fig. 2 and is plotted in Fig. 6. Inset (a) of Fig. 6 shows the variation of the cluster diameter as a function of doping for ZFC samples. Inset (b) reveals the increase in the cluster diameter as the field cooled cluster is exposed to different negative fields showing the depinning of the fluxes from intergranular regions thereby forming bonds. It can be seen that the ZFC susceptibility is larger for larger clusters by comparing inset (a) of Fig. 6 and Fig. 2 which is consistent with the prediction of the model. Further, from our temperature dependence studies¹⁶ we have observed H_m decreasing with increasing T and vanishing near T_c . That is to say the average cluster size diverges to infinity as the percolation threshold is approached from below.

The calculated cluster diameter, however, is very much smaller than the grain diameter ($\sim 10\text{--}6\mu\text{m}$) observed by SEM.⁷ Blazey *et al.*² have also observed this discrepancy and suggested that the area S determines the uniform phase. We have observed twins⁷ within the grains by SEM. Thus, comparing these sizes of uniform phase and the grain we can say that the coupling is within the grain. Thus, clusters may be formed through different grains or within the grains.

All the parameters studied as a function of the cooling field (Figs. 2 and 3) substantiate the fact that the difference between ZFC and FC signals appears only for

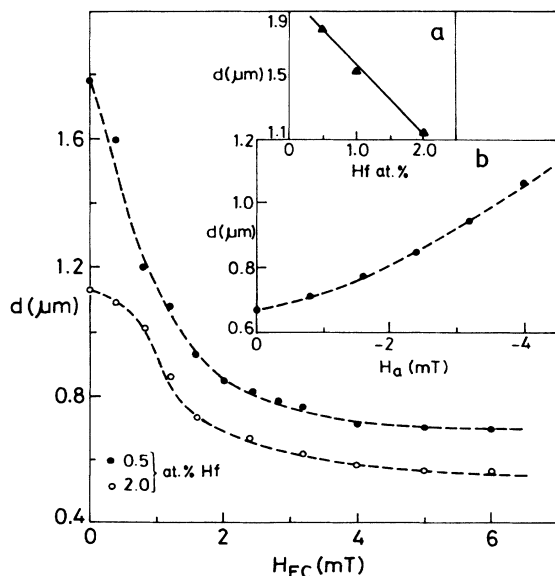


FIG. 6. Calculated superconducting cluster diameter d from the relation $S = \phi_0 / 2H_{c1}^*$ using $H_m \approx H_{c1}^*$ (from the inset of Figs. 2 and 5).

fields greater than H_m (or H_{c1}^*). Therefore, glassy behavior can be expected in ceramics for fields greater than or equal to H_{c1}^* . This observation is very consistent with the predictions of Aksenov and Sergeenkov²¹ who have calculated the phase diagram for a superconducting glass model. According to them, the Meissner phase exists up to fields equal to H_0 ($H_0 \approx H_m$ or H_{c1}^*) and superconducting glass phase appears for $H_0 < H < H_u$ where $H_0 = \phi_0 / 2S$ and $H_u \approx 15H_0$. Their calculated FC magnetization is exactly similar to our observed variation of h_p (Fig. 2). However, Morganstern¹⁴ has proposed the range 0.03–0.2 T to observe the glass phase, and the glass concept can be understood as a generalization of the traditional flux-creep picture. His range of temperature (95%–70% T_c) to observe the glassy behavior is consistent with our observations.

Finally, from these studies we calculate some of the parameters for the sake of comparison with the literature. In the limit where the grain diameter $R_g \gg \lambda_g$ ($\approx \lambda_x \approx \lambda_z \approx 0.2\mu\text{m}$ for ceramics), the intergrain penetration depth is given by¹⁵ $\lambda_j = (\phi_0 / 2\pi\mu J_0 a)^{1/2}$, where J_0 is the intergrain current density and $J_0 = I_0 / a^2$ (I_0 is the tunneling current). In our samples, grain size decreases⁷ from 10 to 6 μm as Hf doping was increased from 0.5 to 2 at. % and their normal state resistance increased from 1.8 to 2.3 m Ω and is linear with doping. Therefore we have assumed $I_0 \approx 100\text{--}75\mu\text{A}$ which is inversely proportional to their normal state resistances. Then, estimated J_0 varies from 100–210 A/cm² for 0.5–2 at. % Hf doping. Also, for $R_g \gg \lambda_g$, $\mu \approx f_n$, where f_n is the normal (intergranular) volume fraction and we have taken f_n varying from 0.2–0.35 proportional to the doping. Calculated λ_j varies from 12.8 to 8.6 μm for 0.5–2 at. % Hf doping. This agrees very well with the behavior predicted by the relation²² $\lambda_j = \phi_0 / 4\pi\lambda_L H_{c1j}$, where $H_{c1j} \approx H_m$ and $H_{c1j} \sim 1/a$. However, the calculated λ_j from this relation gives lower estimation, but the behavior is the same. All these values are very much in agreement with the accepted literature values. Further, according to the model²³ for the effect of grain boundaries on magnetic field penetration, the parameter $(\lambda_z / \lambda_j)^2$ determines the coupling strength. We have taken λ_z as 0.2–0.3 μm proportional to their normal state resistances and calculated λ_j s to estimate $(\lambda_z / \lambda_j)^2$ which varies from 2.44×10^{-4} to 16.5×10^{-4} in good agreement with the model which predicts stronger coupling with decreasing grain size. This is further supported by the observed increase in the decoupling field with decreasing grain size.

In conclusion, we have clearly demonstrated the flux trapping during FC process using a sensitive probe, the microwave absorption, in doped ceramic samples. Glass phase appears at a much lower field, that is for fields greater than or equal to H_{c1}^* . The observed glassy behavior is the consequence of weak links at grain boundaries or at twin boundaries. As the calculated superconducting cluster size is much lower than the grain size observed by SEM, it is clear that the superconducting loop is formed within the grains or through different grains choosing a proper ground state to satisfy the requirements of the flux quantization. Percolation description

along with the superconducting cluster model of Ebner and Stroud qualitatively explains the observed results.

ACKNOWLEDGMENTS

We would like to thank V. N. Moorthy, C. V. N. Rao, Prem Chand and Md. Shahbuddin for their kind help,

and Dinesh Kanojia for his technical assistance. The financial support of Department of Science and Technology, New Delhi and the Council for Scientific and Industrial Research (India) (CSIR), New Delhi is gratefully acknowledged.

-
- ¹K. Kachaturyan, E. R. Weber, P. Tejedor, A. M. Stacy, and A. M. Portis, *Phys. Rev. B* **36**, 8309 (1987).
- ²K. W. Blazey, K. A. Müller, J. G. Bednorz, W. Berlinger, G. Amoretti, R. Buluggiu, A. Vera, and F. C. Matocotta, *Phys. Rev. B* **36**, 7241 (1987).
- ³S. V. Bhat, P. Ganguly, T. V. Ramakrishnan, and C.N.R. Rao, *J. Phys. C* **20**, L 559 (1987).
- ⁴R. S. Rubins, J. E. Drumheller, S. L. Hutton, S. V. Rubanecker, B. Y. Jeong, and T. D. Black, *J. Appl. Phys.* **64**, 1312 (1988), and references therein.
- ⁵E. J. Pakulis and T. Osada, *Phys. Rev. B* **37**, 5940 (1988).
- ⁶A. Gould, E. M. Jackson, R. Renouard, R. Crittenden, S. M. Bhagat, N. D. Spencer, L. L. Dolhert, and R. F. Wormsbecher, *Physica C* **156**, 555 (1988).
- ⁷A. G. Vedeshwar, Md. Shahbuddin, Prem Chand, H. D. Bist, S. K. Agarwal, V. N. Moorthy, C. V. N. Rao, and A. V. Narlikar, *Physica C* **158**, 385 (1989).
- ⁸K. W. Blazey, A. M. Portis, and J. G. Bednorz, *Solid State Commun.* **65**, 1153 (1988), and references therein.
- ⁹M. Warden, M. Stadler, G. Stafanicki, A. M. Portis, and F. Waldner, *J. Appl. Phys.* **64**, 5800 (1988), and references therein.
- ¹⁰K. A. Müller, M. Takashige, and J. G. Bednorz, *Phys. Rev. Lett.* **58**, 1143 (1987).
- ¹¹E. V. Blinov *et al.*, *Pis'ma Zh. Eksp. Teor. Fiz.* **48**, 147 (1988) [*JETP Lett.* **48**, 159 (1988)].
- ¹²Y. Yeshurun and A. P. Malozemoff, *Phys. Rev. Lett.* **60**, 2202 (1988).
- ¹³C. Giovannella, C. Chappert, P. Beauvillain, and G. Collin, *Int. J. Mod. Phys.* **1**, 1011 (1987).
- ¹⁴I. Morganstern, *IBM J. Res. Develop.* **33**, 307 (1989).
- ¹⁵J. R. Clem, *Physica C* **153-155**, 50 (1988).
- ¹⁶A. G. Vedeshwar *et al.*, *Phys. Lett. A* **139**, 415 (1989).
- ¹⁷G. Deutscher, O. E. Wohlman, S. Fishman, and Y. Shapira, *Phys. Rev. B* **21**, 5041 (1980); O. E. Wohlman, A. Kapitulnik, and Y. Shapira, *ibid.* **24**, 6464 (1981).
- ¹⁸S. John and T. C. Lubensky, *Phys. Rev. Lett.* **55**, 1014 (1985); *Phys. Rev. B* **34**, 4815 (1986); **38**, 2533 (1988).
- ¹⁹W. Y. Shih, C. Ebner, and D. Stroud, *Phys. Rev. B* **30**, 134 (1984); C. Ebner and D. Stroud, *ibid.* **31**, 165 (1985).
- ²⁰K. Härkönen, I. Tittonen, J. Westerholm, and K. Ullakko, *Phys. Rev. B* **39**, 7251 (1989).
- ²¹V. L. Aksenov and S. A. Sergeenkov, *Physica C* **156**, 18 (1989); **156**, 235 (1989).
- ²²K. W. Blazey, A. M. Portis, and F. H. Holtzberg, *Physica C* **157**, 16 (1989).
- ²³T. L. Hylton and M. R. Beasley, *Phys. Rev. B* **39**, 9042 (1989).